ELSEVIER

Ceramics International 29 (2003) 311–316

CERAMICS INTERNATIONAL

www.elsevier.com/locate/ceramint

Mechanical properties and thermal shock behaviour of alumina–mullite–zirconia and alumina–mullite refractory materials by slip casting

Cemail Aksel*

Department of Material Science and Engineering, Anadolu University, Iki Eylül Campus, 26555 Eskisehir, Turkey

Received 30 April 2002; accepted 31 May 2002

Abstract

Strength and modulus values of slip-cast alumina–mullite–zirconia and alumina-mullite refractories have been determined as a function of quench temperature by air and water quenching. The resistance to fracture initiation and propagation caused by the thermal stresses was increased with the addition of zircon, as supported by the R and R_{st} parameters. There was no catastrophic decline in strength on thermal shock at high temperature or with repeated cycling, where a large proportion of intergranular fracture in the fracture surfaces was observed. There was ~50% loss of strength after the 1st cycle, and further cycling did not markedly change the retained strength of the material to the 40th cycle. The inevitable cracking occurred after thermal shock testing was kept below the critical crack length due to the transformation toughening effect of zirconia, thus maintaining a high degree of integrity, associated with the high values of K_{1c} and γ_i.

Keywords: A. Slip casting; C. Mechanical properties; D.Mullite; D. Al_2O_3; D. ZrO_2; E. Refractories; Thermal shock

1. Introduction

Alumina–mullite–zirconia (AMZ) and alumina–mullite (AM) expendable refractories are widely used in the forehearth, distributor, feeders, and glass melting furnaces, as plungers, spouts, tubes, stirrers, channels, rotor segments, mantle blocks, and orifice rings [1,2]. AMZ refractory materials, composed of mullite and dispersed ZrO_2 particles, show a better thermal shock resistance than other AMZ and AM materials, and even than pure mullite [3]. AMZ refractory materials at room temperature show a high strength and fracture toughness [4,5], but these properties decrease significantly at high temperature because of glassy phase in the grain boundaries [6].

The starting decomposition temperature of zircon is about 1675 °C according to the ZrO_2–SiO_2 phase diagram [7]. The existence of some impurities in the starting powder can be lowered the decomposition temperature conspicuously [8]. During reaction bonding, the zircon dissociation and mullite formation commence at ~1400 °C and are practically completed by 1500 °C [9]. The radial decomposition of zircon starts from the surface to the centre of the grain, which leads to rapid crystallisation of zirconia and to the formation of amorphous silica [10]. The presence of a glassy phase at some of the triple junctions will initiate at high temperatures, which is responsible for the decrease of strength of zircon at high temperature [8].

In thermal shock test by air quenching (strength as a function of the number of cycle), a material containing zirconia maintains a complete and solid body with a few cracks after 30 cycles, with 50% strength loss [11]. Cracking must have occurred during cooling from 1000 °C accompanying a significant amount of volume expansion [11]. On the contrary, cracking occurred due to thermal expansion mismatch might be considerably diminished by crack healing as the temperature increases due to the presence of a glassy phase [3].

A number of parameters defined by Hasselman [12] can be used to predict the thermal shock behaviour of a material. The most widely used of these are the R, and

* Tel.: +90-222-3350580 x6355; fax: +90-222-3239501.
E-mail address: caksel@anadolu.edu.tr (C. Aksel).

0272-8842/03/$22.00
PII: S0272-8842(02)00139-6

R_{st}. R predicts the resistance of a material to the initial shock and is expressed as the difficulty of crack initiation. R is given by the formula, $\{R=[\sigma_f\ (1-\nu)]/(E\alpha)\}$, where σ_f is strength, E is Young's modulus, ν is Poisson's ratio and α is the mean thermal expansion coefficient of the composite. α values of refractories, depending on the Young's modulus, volume fraction and coefficient of thermal expansion of each component, can be calculated from the equation derived by Turner [13]. If strength is high and Young's modulus and coefficient of expansion are low, a material will therefore have a high resistance to crack initiation. However, once a crack has been initiated, the controlling feature of thermal shock failure then becomes the nature of crack propagation through the material [14]. $R_{st}=[\gamma_i/(\alpha^2.E)]^{1/2}$ parameter [12] can be used to determine the maximum allowable temperature difference required to propagate long cracks under severe thermal stress conditions, where γ_i is a measure of resistance to the initiation of crack propagation. In both cases a high value would indicate good resistance to thermal stresses. Although a brittle material with very high strength would be resistant to crack initiation, once the stress had exceeded the fracture strength of that material, failure would be sudden and catastrophic. On the other hand, if crack initiation occurred at moderate stress levels, but those cracks were then prevented from propagating through the material, thermal shock resistance would be equally good provided adequate strength was retained in the piece. Since most refractories are composed of brittle, multigranular oxides, crack initiation takes place with ease; adequate thermal shock is then achieved by controlling the R_{st} parameter through microstructural features such as porosity and crack stability. So that further weakening of a refractory material with increasing severity of thermal shock can be predicted by R_{st}. It must be realised that the Hasselman parameters are simply predictions of behaviour, to have any practical value they must be capable of confirmation by some independent tests.

Thermal shock testing has been traditionally carried out by quenching samples from a predetermined temperature into air, water or oil, followed by reheating in a kiln. The first step in testing is to determine the critical quench temperature, ΔT_c, which can be defined as the minimum temperature required to produce cracking. Further testing below this critical temperature would not cause damage and would therefore be pointless. Cycling in this manner is carried out until total failure of the piece occurs. This method is rather subjective and, at its best, is only really suitable for comparative data. Strength testing after each thermal cycle will give the data required, and, when combined with the determination of critical quench temperature and fracture toughness, an overall picture of the material's behaviour under thermal stress can be built up.

AMZ refractories used in the glass industry are subject to thermal shock stresses during installation. Once installed, the service life of the refractory is then determined for the most part by its corrosion characteristics. AMZ expendables are recognised as having excellent thermal shock characteristics being able to withstand >40 cycles in the laboratory test without visible damage. This paper offers an explanation of this behaviour by examining the microstructure and fracture surfaces of samples, associated with the mechanical properties of slip cast AMZ and AM refractory materials under a variety of thermal shock conditions.

2. Experimental procedure

AMZ composition containing ~20% zircon (sample A), and the other batch without zircon (sample B), whilst keeping the AM ratio constant (~3:1), were prepared by slip casting. Slips were taken and cast into bars 150×10×15 mm. Samples were then dried in an oven at ~110 °C to reduce the effect of possible significant amount of shrinkage. After firing, bulk density and apparent porosity values were measured using the standard water immersion method [15]. Mechanical properties of those bars have been determined at room temperature. Then, critical quench temperature was determined by heating the bars from room temperature to 1400 °C; quenching five bars each in air and water at 200 °C intervals. These were tested using a Mayes, SMT50 tensile testing machine in three-point configuration with a support roller span of 115 mm, at a crosshead speed of 1 mm min^{-1}. Using the standard equations for the strength (σ) [16] and Young's Modulus (E) [17], these values were determined and the average taken for each quench temperature.

$$\sigma = (3/2).(P\ L)/\left(W\ D^2\right) \qquad E = L^3\ m/\left(4\ WD^3\right) \qquad (1, 2)$$

where P is the load at fracture, L is the length of support span, W is the specimen width, D is the specimen thickness, and m is the slope of the tangent of the initial straight-line portion of the load-deflection curve. Fracture toughness was then measured using the single edge notched beam (SENB) technique [18], with a (6 mm deep) notch cut with a 1 mm thick diamond blade producing a notch to depth ratio of 0.25. Fracture toughness (K_{1c}) was then calculated from the maximum load using Eq. (3):

$$K_{1c} = (3/2).\left(P\ Lc^{1/2}\right).Y/\left(W\ D^2\right) = (2E\gamma_i)^{1/2} = \left(\sigma\ Y\ C^{1/2}\right) \qquad (3, 4, 5)$$

where c is the notch depth, γ_i is a measure of resistance to the initiation of crack propagation, C is the critical

crack length and $Y=[A_0+A_1(c/D)+A_2(c/D)^2+A_3(c/D)^3+A_4(c/D)^4]$. Y is a dimensionless number, which is dependent on the geometry of the loading and the crack configuration with $L/D\approx 8$, $A_0=+1.96$, $A_1=-2.75$, $A_2=+13.66$, $A_3=-23.98$, $A_4=+25.22$ [18].

Thermal shock parameters R and R_{st} were then calculated in order to predict thermal shock behaviour of those samples. Cyclic thermal shock testing was carried out at 1000 °C (above the critical temperature) by water quenching to a maximum of 40 cycles. Five bars were taken for strength testing at the 1st and 2nd cycles, and then every 5th cycle to 20 cycles and finally every 10th cycle. By using a CamScan 4 scanning electron microscope, back scatter and secondary electron images were then made to examine the microstructure and fracture surfaces of samples.

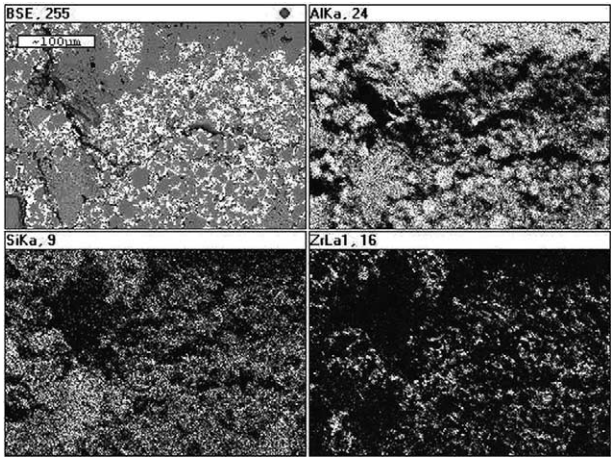

Fig. 1. Map distribution of the AMZ refractory.

3. Results and discussion

The density and apparent porosity values of samples were 3.0 g cm^{-3} and 19% for A, and 2.7 g cm^{-3} and 23% for B, respectively. The presence of zircon promoted the densification and thus reduced the porosity significantly, which was considered to be as an important factor for the increase in mechanical properties. Mechanical properties of the AMZ and AM refractory materials prepared by slip casting are presented in Table 1. It has been found that removing zirconia from the AMZ refractory composition whilst keeping the alumina:mullite ratio constant, reduces the strength, Young's modulus and fracture toughness by a factor of ~2.4 and the fracture surface energy by a factor of 2.7. Knowledge of the fracture toughness and strength also allows the calculation of critical crack length (C) from Eq. (5), which is the crack length beyond which there is no arresting of cracks, propagation takes place with ease and the material loses strength. As can be seen from Fig. 1, the observed crack length for the AMZ refractory material was in general <0.5 mm, which was much smaller than the value of calculated critical crack length, 1.3 mm (Table 1). This is because a volume increase takes place and shear strains develop, which together absorb energy from the crack, thereby preventing the crack length from extending to the critical crack length. As predicted from the R parameter, material containing zirconia appeared to have higher thermal stress resistance with temperature gradients up to ~200 K, showing high resistance to crack initiation (Table 1). In addition, R_{st} parameter also supported that sample A would show a significant improvement (by a factor of ~3.5) in the maximum allowable temperature difference required to propagate long cracks under severe thermal stress conditions, in comparison with sample B (Table 1). It would be expected on the basis of the R and R_{st} parameters to show a high resistance to fracture initiation and propagation caused by the thermal stresses in consequence of the presence of zircon.

Zircon appears to be the controlling factor in mechanical properties, because of thermal contraction mismatch between the phases, and volume expansion associated with zirconia transformation and mullite formation. The significant improvement in K_{1c} value of sample A can be correlated to increase in the fracture surface energy (γ_i) due to a reduction of crack tip stress intensity in the plastic zone ahead of the crack, by energy dissipation through relaxation occurring in the grain boundary phase.

Scanning electron microscopy shows that there were mostly intergranular, with some transgranular, cracks after strength testing prior to thermal shocking the samples (Fig. 2a); however, samples quenched from 1200 °C showed a large proportion of intergranular fracture (Fig. 2b). This change in fracture path to a marked intergranular fracture with increasing quench temperature, is thought to be the main reason for the increase in fracture surface energy required to initiate crack. Therefore, more fracture surface energy was

Table 1
Mechanical properties and thermal shock parameters of AMZ and AM refractories

Sample	σ (MPa)	E (GPa)	K_{1c} (MPa m$^{1/2}$)	C (mm)	γ_i (J m^{-2})	R (K)	R_{st} (m$^{1/2}$ K$^{1/2}$)
A	16.5±1.5	15.2±2.2	1.2±0.1	1.3±0.2	44.3±0.2	191±32	2.7±0.2
B	6.8±0.6	6.5±0.7	0.5±0.1	1.1±0.1	16.3±0.2	102±6	0.8±0.0

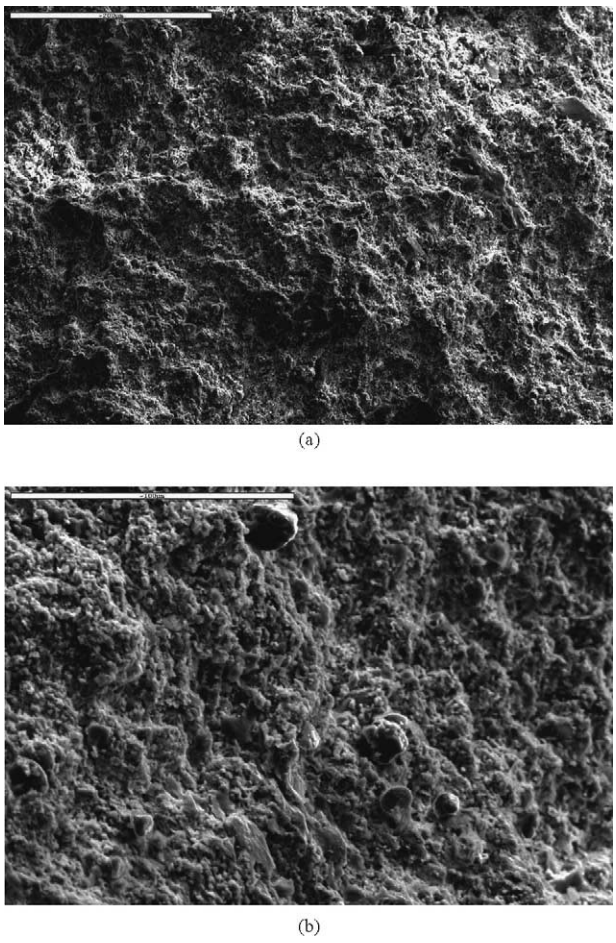

Fig. 2. Fracture surface of the AMZ refractory: (a) at 25 °C (scale bar: 200 μm), (b) after water quenching at 40th cycle (scale bar: 100 μm).

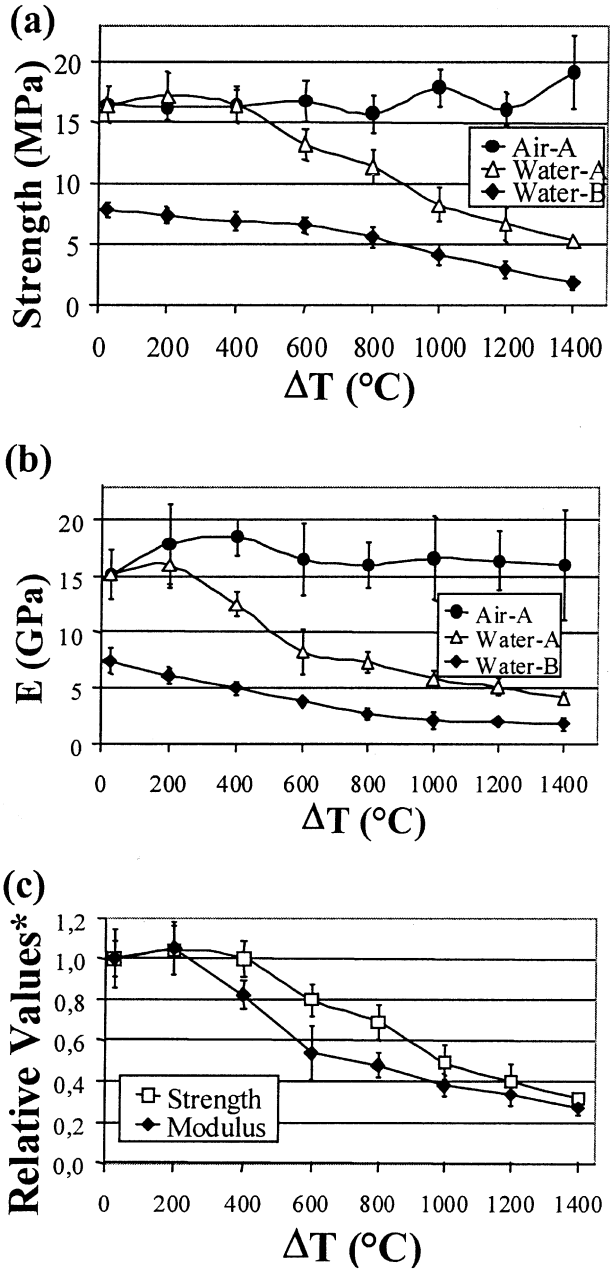

Fig. 3. Mechanical properties of the refractories, as a function of quench temperature: (a) strength, (b) Young's modulus, (c) fraction of initial strength and modulus values* of the AMZ refractory.

required in AMZ refractory materials to connect the cracks for propagation. This can be attributed to high K_{1c} value of the AMZ refractory material, indicating high resistance to fracture of a material, which is supported by the R and R_{st} parameters (Table 1).

After calculating thermal shock parameters R and R_{st}, the behaviour of materials was predicted on that basis, and these predictions were compared with the experimental thermal shock test data. Fig. 3a shows the determination of critical quench temperature. It can be seen that the strength remained relatively constant throughout the range indicating that little or no damage was being done to the material by air quenching. Under the more severe thermal shock of the water quench, the strength decreased gradually as the quench temperature rose. The implication of this result is that as the quench temperature is increased, the number of cracks initiated in the sample also increases, hence the gradual decline in strength. It should also be noted that under water quench conditions, there was no significant decline in strength until the quench temperature was >400 °C for sample A and >600 °C for sample B; this is evidence for the existence of microcracking in the sample after initial firing. This is an inevitable consequence of mismatch in thermal expansion coefficients of the constituent phases in the material and the possibility of phase transformations in the zirconia. For example the coefficients of thermal expansion are, $\sim$8.2 MK^{-1} for alumina, $\sim$5.1 MK^{-1} for mullite and $\sim$7.6 MK^{-1} for zirconia [19,20], whilst the tetragonal to monoclinic phase transformation of zirconia which takes place at $\sim$1000 °C is generally

regarded as giving a ~5% to expansion, but will only do so if there is sufficient elasticity or space to accommodate this expansion. The development of a microcrack on thermal shock gives this necessary space for the transformation to occur and in so doing actively prevents the propagation of the crack by leading to a transformation zone which surrounds the crack, as a result of the transformation toughening mechanism.

Young's modulus values (Fig. 3b) confirm these findings showing that there was no crack propagation observed by air quenching. However, none of these cracks actually reach the critical size at which catastrophic failure would occur. There is evidence here that the microcracking increased from 200 to >600 °C by water quenching, resulting in a 50% reduction in Young's modulus over this range. Increasing the severity of the shock beyond this point gave only a marginal decrease in modulus up to 1400 °C. The significant incline (>2) in modulus of sample A, at the maximum quench temperature used, with the addition of zircon indicated a higher resistance to microcrack propagation, and therefore better thermal shock resistance than that of sample B.

Furthermore, these effects are shown more clearly in Fig. 3c, where fraction of initial strength and modulus data (e.g. after quenching relative to initial values) are given with respect to quench temperature. Since many refractory materials fail suddenly and catastrophically when thermally shocked beyond the critical temperature there is clearly an important mechanism involved here which results in the AMZ refractory retaining a good proportion of its strength and modulus far beyond that point. The calculated R and R_{st} parameters for those refractory materials showed a good correlation with the fraction of initial strength and modulus values after thermal shock testing. It has been confirmed that thermal stress resistance parameters, R and R_{st}, can be used to characterise thermal shock damage of those refractory materials for an industrial applications. The effect of the porosity on mechanical properties and thermal shock behaviour must also be taken into account in characterising and determining the service performance of slip-cast refractory materials.

Fig. 4 shows that there was approximately 50% loss of strength after the 1st cycle. Subsequent cycling did not significantly alter the retained strength of the material to the 40th cycle. Fracture surface of sample A subjected 40 cycles by water quenching showed an intergranular fracture path similar to that of the 1st cycle (Fig. 2b). The fracture of the AMZ material is semi-stable, but never catastrophic. This can be attributed to high values of γ_i, indicating that more fracture energy is required to connect the cracks for propagation, and K_{1c}, showing higher resistance to fracture of a material.

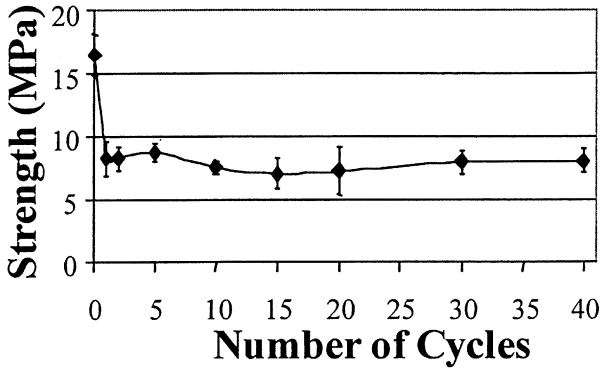

Fig. 4. Strength of the AMZ refractory, as a function of number of cycles, by water quenching at 1000 °C.

4. Conclusions

The incorporation of zircon powder into the aluminosilicate refractory provided more improvement in strength through a reduction in porosity by void filling and by faster sintering with the improvement of interparticle bond strength, leading to high-density values. AMZ refractory material showed a high resistance to crack initiation and propagation, which was supported by the thermal shock parameters. There was no catastrophic decline in strength on thermal shock at high temperature or with repeated cycling. The prominence of intergranular cracking observed following thermal shock is indicative of a high value of the amount of energy required to initiate crack propagation and is attributable to the high value of K_{1c}. Crack propagation is limited to short distances through the material due to the transformation toughening effect of zirconia. The inevitable cracking, which does occur on thermal shock, is kept below the critical crack length, thus maintaining a high degree of integrity. These results confirm the AMZ refractory material to be highly resistant to thermal shock in severe environments.

Acknowledgements

The author wishes to thank Professor F.L. Riley and Mr. F. Konieczny for their helpful discussions, and their invaluable expertise in this field was greatly appreciated.

References

[1] D.E. Parkinson, Feeder and forehearth refractories, Glass Technology 29 (5) (1988) 173–176.
[2] C. Aksel, F. Konieczny, Mechanical properties and thermal shock behaviour of PSR-333 alumina–mullite–zirconia refractory material, Glass International 24 (1) (2001) 16–18.
[3] G. Orange, G. Fantozzi, F. Cambier, C. Leblud, M.R. Anseau, A. Leriche, High temperature mechanical properties of reaction-sintered mullite/zirconia and mullite/alumina/zirconia composites, J. Mater. Sci. 20 (1985) 2533–2540.

[4] H.M. Jang, S.M. Cho, K.T. Kim, Alumina–mullite–zirconia composites, part II, microstructural development and toughening, J. Mater. Sci. 32 (2) (1997) 503–511.
[5] A.C. Mazzei, J.A. Rodrigues, Alumina–mullite–zirconia composites obtained by reaction sintering: part I. Microstructure and mechanical behaviour, J. Mater. Sci. 35 (11) (2000) 2807–2814.
[6] T. Koyama, S. Hayashi, A. Yasumori, K. Okada, M. Schmucker, H. Schneider, Microstructure and mechanical properties of mullite/zirconia composites prepared from alumina and zircon under various firing conditions, J. Eur. Ceram. Soc. 16 (2) (1996) 231–237.
[7] B.O. Mysen, Phase Diagrams for Ceramists, National Institute of Standards and Technology, The American Ceramic Soc. 8 (1990) 188.
[8] Y. Shi, X.X. Huang, D.S. Yen, Fabrication of hot-pressed zircon ceramics: mechanical properties and microstructure, Ceram. Int. 23 (5) (1997) 457–462.
[9] S. Lathabai, D.G. Hay, F. Wagner, N. Claussen, Reaction-bonded mullite/zirconia composites, J. Am. Ceram. Soc. 79 (1) (1996) 248–256.
[10] F. Cambier, C.B. Delalastra, P. Pilate, A. Leriche, Formation of microstructural defects in mullite–zirconia and mullite–alumina–zirconia composites obtained by reaction-sintering of mixed powders, Trans. J. Br. Ceram. Soc. 83 (6) (1984) 196–200.
[11] K.J. Chen, Y.C. Ko, Evaluation of zirconia refractories for continuous-casting, Am. Ceram. Soc. Bull. 62 (9) (1983) 1030–1035.
[12] D.P.H. Hasselman, Thermal stress resistance parameters for brittle refractory ceramics: a compendium, Am. Ceram. Soc. Bull. 49 (12) (1970) 1033–1037.
[13] P.S. Turner, Thermal-expansion stresses in reinforced plastics, J. Res. Natl. Bur. Stand. 37 (4) (1946) 239–250.
[14] R.C. Bradt, Fracture testing of refractories, past present and future, in: Proc. 2nd Int. Conf. on Refractories, Refractories '87, No. 1, Tokyo, 1987, pp. 61–68.
[15] British Standard Testing of Engineering Ceramics, BS 7134 Section 1.2, 1989.
[16] ASTM C1161–90, Standard test method for flexural strength of advanced ceramics at ambient temperature, Annual Book of ASTM Standards, 15.01, 1991, pp. 327–333.
[17] ASTM D790M-86, Standard test methods for flexural properties of unreinforced and reinforced plastics and electrical insulating materials, Annual Book of ASTM Standards, 08.01, 1988, pp. 290–298.
[18] W.F. Brown, J.E. Srawley, Plane strain crack toughness testing of high strength metallic materials, ASTM Spec. Tech. Publ., No: 410, 1967, pp. 1–23.
[19] S.J. Burnett, Properties of Refractory Materials, UKAEA Research Group Report, Harwell, 1969.
[20] J.F. Shackelford, W. Alexander, J.S. Park, CRC Materials Science and Engineering Handbook, CRC Press, Boca Raton, FL, 1994.